

ORIGINAL ARTICLE

The Fragile X proteins Fmrp and Fxr2p cooperate to regulate glucose metabolism in mice

Jeannette G. Lumaban and David L. Nelson*

Department of Molecular and Human Genetics, Jan and Dan Duncan Neurological Research Institute, Baylor College of Medicine, 1250 Moursund Street, Houston, TX 77030, USA

*To whom correspondence should be addressed. Tel: +1 832 824 8160; Fax: +1 832 825 1273; Email: nelson@bcm.edu

Abstract

Fragile X syndrome results from loss of *FMR1* expression. Individuals with the disorder exhibit not only intellectual disability, but also an array of physical and behavioral abnormalities, including sleep difficulties. Studies in mice demonstrated that *Fmr1*, along with its paralog *Fxr2*, regulate circadian behavior, and that their absence disrupts expression and cycling of essential clock mRNAs in the liver. Recent reports have identified circadian genes to be essential for normal metabolism. Here we describe the metabolic defects that arise in mice mutated for both *Fmr1* and *Fxr2*. These mice have reduced fat deposits compared with age- and weight-matched controls. Several metabolic markers show either low levels in plasma or abnormal circadian cycling (or both). Insulin levels are consistently low regardless of light exposure and feeding conditions, and the animals are extremely sensitive to injected insulin. Glucose production from introduced pyruvate and glucagon is impaired and the mice quickly clear injected glucose. These mice also have higher food intake and higher VO_2 and VCO_2 levels. We analyzed liver expression of genes involved in glucose homeostasis and found several that are expressed differentially in the mutant mice. These results point to the involvement of *Fmr1* and *Fxr2* in maintaining the normal metabolic state in mice.

Introduction

Fragile X syndrome (FXS) is the most frequent cause of inherited intellectual disability, affecting ~1 in 4000 males and 1 in 8000 females (1,2). The most common mutation in FXS is a CGG repeat expansion that results in the silencing of the *Fragile X Mental Retardation 1* (*FMR1*) gene (3). *FMR1* encodes the protein FMRP, which with its paralogous proteins FXR1P and FXR2P forms the fragile X-related protein family (Fragile-X related or FXR). These RNA-binding proteins share >60% amino acid identity, are co-expressed in many tissues, interact with one another and function to regulate translation and stability of numerous RNA targets (4–9).

Apart from moderate to severe intellectual disability, males with fragile X syndrome display physical and behavioral abnormalities, including a long, narrow face, large ears, macroorchidism, hyperactivity and autistic-like behaviors. A fraction of fragile X males also presents with disordered sleep (10–13). Both fruit flies and mice lacking *Fmr1* exhibit altered circadian

behaviors (14–16). Some fragile X males also exhibit a 'Prader-Willi-like phenotype' with apparently altered metabolic status leading to hyperphagia and obesity (17, 18). Variation in the phenotypes of individuals with fragile X syndrome may stem from variable compensation by FXR family members.

Our prior efforts to identify areas of potential compensation by FXR family members in *Fmr1* KO mice identified enhanced phenotypes when both *Fmr1* and *Fxr2* were mutated. Double knockout mice have enhanced behavioral phenotypes and a significant anomaly in the long term depression response of the hippocampus to the mGluR5 agonist (S)-3,5-dihydroxyphenylglycine (19, 20). We also found significantly altered circadian activity that was not responsive to light–dark cues (16). We found that the absence of *Fmr1* and *Fxr2* also altered mRNA levels and cycling of both *Bmal1* and *Npas2* in liver, suggesting disruption of the regulatory loop that is central to maintenance of circadian rhythm in this tissue (16). These essential clock component genes have been shown to regulate metabolism, playing an

important role in maintaining glucose homeostasis by adjusting metabolic processes to daily feeding–fasting cycles (21–25).

Since the absence of *Fmr1* and *Fxr2* alters circadian rhythm and regulated expression of essential clock components, we sought to determine whether these proteins are also involved in glucose homeostasis. The small fraction of individuals with FXS who exhibit the Prader–Willi phenotype do not have cytogenetic or methylation abnormalities characteristic of Prader–Willi syndrome (17,18,26,27). Apart from these individuals, fragile X patients are typically not tested for metabolic defects and thus other, more subtle alterations in metabolism may be present. Analyses in model systems have the potential to reveal phenotypes that have gone undetected due to variable expression among patients. Several other intellectual disability disorders that also have circadian problems—such as Smith–Magenis syndrome and Down syndrome—are known to have symptoms relating to metabolism perturbances (28–33).

Our studies reveal that the absence of *Fmr1* and *Fxr2* significantly alters glucose homeostasis. Mice lacking both *Fmr1* and *Fxr2* have significantly lower body fat than age- and weight-matched controls and show altered circadian variation of metabolic markers. These mice are also very sensitive to insulin, have impaired glucose production and exhibit quicker clearance of introduced glucose. While very lean, *Fmr1/Fxr2* double knockout (DKO) mice exhibit higher food intake compared with wild-type (WT) mice, even as their metabolic rate remains comparable. In a screen of genes involved in glucose homeostasis, we found differential expression not only between WT and DKO, but also between fasted and fed mice, regardless of genotype. Our data suggest that dysregulation of circadian regulation in liver and possibly other tissues in DKO animals leads to significant alteration of their metabolism.

Results

Fmr1/Fxr2 DKO mice exhibit lower total body fat

As an initial test of the metabolic state of the animals, we measured body composition of age-matched male mice using EchoMRI. While body weight is comparable between all five genotypes studied (WT, *Fmr1* KO, *Fxr2* KO, *Fmr1/Fxr2* DKO, and *Fmr1* KO/*Fxr2* het [KOH]), both *Fxr2* KO and DKO mice show significantly lower total body fat (Fig. 1A and B). Consequently, these mice also had a higher percentage of lean mass compared with the WT mice (Fig. 1C). This would indicate that deficiency in the *Fxr2* gene affects adipose tissue deposition in mice, but the absence of *Fmr1* does not appear to be a significant factor in whole body composition.

Circadian variation of metabolic markers in circulating blood is disrupted in DKO mice

To determine whether lack of either or both *Fmr1* and *Fxr2* would affect the circadian variation of common metabolic markers, we collected plasma over 24 h at four time points (ZT0, ZT6, ZT12 and ZT18 where ZT0 = 7 AM when lights are first turned on) from mice that were maintained in a 12:12 light–dark (LD) cycle. Plasma samples were analyzed for glucose, insulin, leptin, cholesterol, adiponectin, triglycerides, free fatty acids and glycerol. As expected, both plasma glucose and insulin were subject to circadian variation in WT mice, peaking at either 1 AM or 7 AM, when the lights have been off and the mice are most active and presumably feeding (Fig. 2A and B). In contrast, with the exception of triglycerides, all the metabolic markers show little to no oscillation in the *Fmr1/Fxr2* DKO mice (Figs 2 and 3), and their glucose levels are significantly lower than those of WT mice at 7 AM, while insulin levels are lower at both 7 AM and 1 AM (Fig. 2A and B). This lack of oscillation is even more pronounced for leptin and cholesterol, where the measured amounts for the DKO mice, along with those of the *Fxr2* KO mice, show little change over the course of the day and are significantly lower than the WT measurements in nearly all time points (Fig. 3A and B). This is expected, as both the *Fxr2* KO and DKO mice have low body fat; leptin is secreted by adipose tissues and in turn regulate the amount of fat stored in the body, among other functions. The DKO mice exhibited normal variation of plasma triglycerides and slight oscillation in levels of adiponectin, free fatty acids and glycerol (Fig. 3C–F), though somewhat out of phase in the latter three measured markers. Levels were significantly different from WT at 7 AM for both free fatty acids and glycerol. Triglycerides are hydrolyzed into free fatty acids and glycerol during lipolysis, a process that is regulated by insulin. With the DKO mice having consistently low levels of insulin, it is not surprising that even with low levels of body fat, these three components of fat breakdown are within fairly normal levels. Unregulated lipolysis may even be contributing to the low body fat measures in these mice.

To test for the effect of light conditions, the same mice were transferred to total darkness and plasma was again collected over the same time points. Food and water were available to the mice during this time. The glucose levels and circadian variations were comparable between the genotypes (Fig. 2C). The insulin levels, while exhibiting a slight oscillation, were consistently and significantly low over 24 h, not just in the DKO mice but also in the *Fmr1* KO and KOH mice (Fig. 2D).

We then tested the effect of food restriction by limiting the availability of food to 7 h between 11 AM and 6 PM. The mice were kept in total darkness for the duration of the experiment,

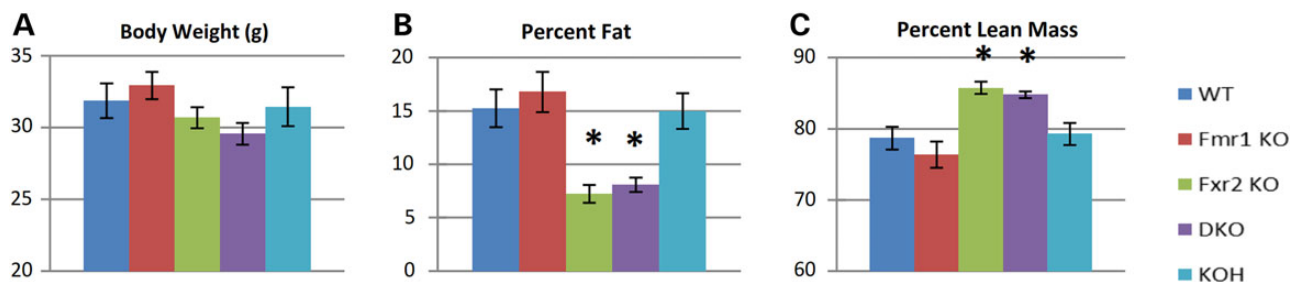


Figure 1. Whole body composition of wild-type (WT), *Fmr1* KO, *Fxr2* KO, *Fmr1/Fxr2* double KO (DKO) and *Fmr1* KO/*Fxr2* het (KOH) mice. MRI was performed on conscious, live mice 5–6 months old using an EchoMRI™ whole body composition analyzer (Echo Medical Systems). While the mice have comparable weights, *Fxr2* KO and DKO mice have significantly lower fractions of body fat and correspondingly higher lean mass compared with WT mice. $N = 11$ – 14 per genotype, values are presented as mean \pm standard error of mean (SEM). Differences were considered significant (*) when $P < 0.05$ compared with WT (two-tailed Student's *t*-test).

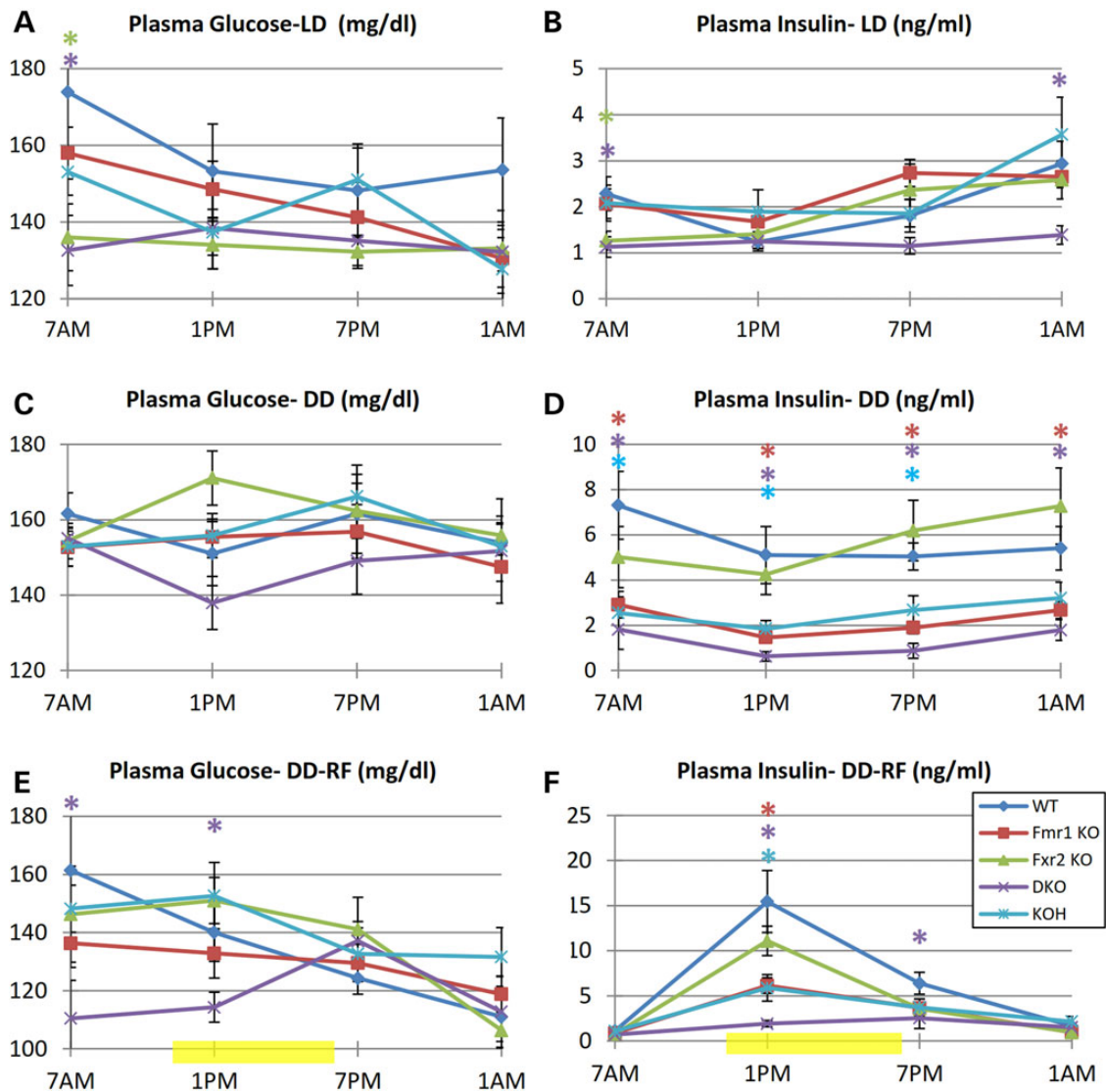


Figure 2. Circadian variation of glucose and insulin under different light and feeding conditions. Male mice 5–6 months old kept at 12:12 LD (7 AM–7 PM), with food available *ad libitum* (A and B). Plasma from blood collected over 24 h at four time points was analyzed for glucose and insulin. Mice are then kept in total darkness (DD), with food available *ad libitum* (C and D) and then challenged with restricted feeding (DD-RF; E and F). On collection days for DD-RF, food is available 11 AM–6 PM (yellow bar). Mice are allowed to recover for a minimum of 5 days between blood collection days. $N = 9–13$ per genotype for A and B, 6–8 per genotype for C–F, values presented as mean \pm SEM. Changes between time points and genotypes determined by ANOVA; pairwise comparisons of each genotype to WT by t-test. Differences were considered significant (*) when $P < 0.05$.

with water available *ad libitum*. Blood was collected on the second day of restricted feeding. Glucose levels displayed circadian variation in all mice, but the DKO mice were out of phase with the other genotypes, peaking at 7 PM when the other mice showed a peak at 7 AM. The glucose values are significantly lower at 7 AM and 1 PM in the DKO compared with WT (Fig. 2E). The presence of an oscillation in glucose levels could be attributed to the presence/absence of food, since this oscillation was not observed in either the LD or the DD experiment where food was available *ad libitum*. The effect of food restriction is even more pronounced in the insulin levels, where all the genotypes displayed a pronounced peaking at 1 PM, the only time point measured during the interval when food was available (Fig. 2F). The DKO mice exhibited very minimal peaking at a significantly lower level compared with WT and still had significantly lower insulin levels at 7 PM when the WT mice already had dropped insulin levels.

The *Fmr1* KO and KOH mice also had lower peak values compared with WT, but their insulin levels remained significantly above those of the DKO mice.

Production of glucose and interplay with insulin is impaired in DKO mice

The low glucose levels in DKO mice led us to investigate the ability of these mice to carry out liver gluconeogenesis from exogenous pyruvate. We measured blood glucose levels at 15, 30, 60 and 120 min after intraperitoneal injection of pyruvate. Both the DKO and KOH mice exhibited impaired rates of gluconeogenesis, measuring significantly lower levels of glucose by 30 min post-injection (Fig. 4A). Glycogenolysis was also tested with injection of glucagon and measurement of glucose levels at the same time points post-injection. While the peak level at 15 min

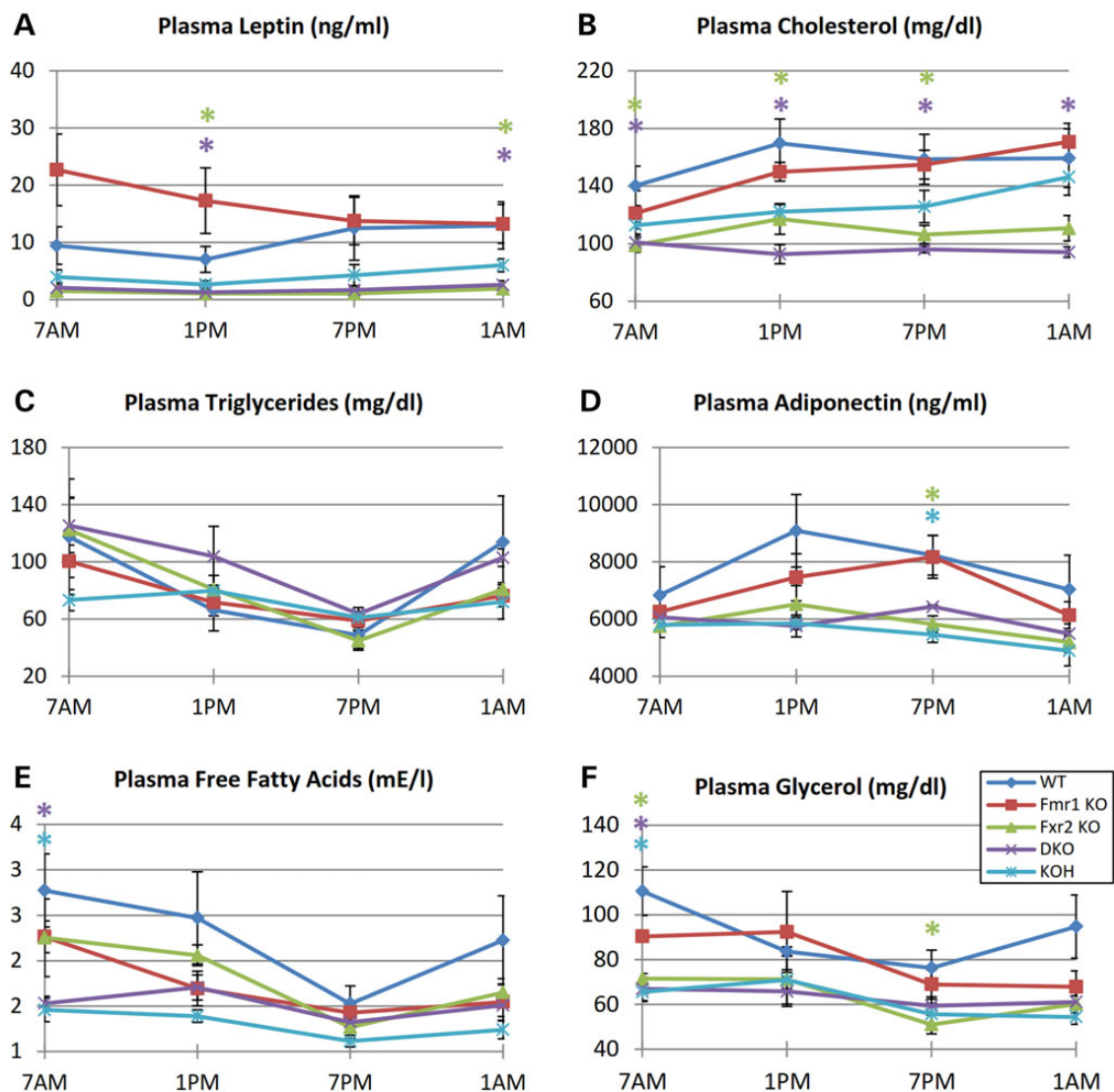


Figure 3. Circadian variation of leptin, cholesterol, triglycerides, adiponectin, free fatty acids and glycerol in circulating blood. Male mice 5–6 months old maintained at 12:12 LD (7 AM–7 PM), with food available *ad libitum*. Plasma from blood collected over 24 h at four time points was analyzed for leptin (A), cholesterol (B), triglycerides (C), adiponectin (D), free fatty acids (E) and glycerol (F). $N = 6–8$ per genotype for A, 3–5 per genotype for B–H, values presented as mean \pm SEM. Changes between time points and genotypes determined by ANOVA; pairwise comparisons of each genotype to WT by t-test. Differences were considered significant (*) when $P < 0.05$.

measurement is significantly lower in the DKO mice, their starting basal glucose level was also lower so that their fold change was comparable to that of the WT (Fig. 4B). Interestingly, the *Fxr2* KO mice had significantly higher glucose levels at 15 min post-injection compared with WT.

When a bolus of glucose was injected intraperitoneally, the DKO mice exhibited significantly lower blood levels compared with WT at all collection time points, including the peak time of 15 min post-injection, even taking into account the lower starting point for DKO (Fig. 4C). This suggests that the DKO mice have an increased efficiency in clearing glucose. The corresponding insulin levels after injection of glucose display very little change over time in DKO mice, and each time point measurement is significantly lower in the DKO compared with WT (Fig. 4D). It is also noteworthy that except for the 15 min post-injection time, insulin levels of the *Fxr2* KO mice are significantly lower compared with WT, even though their glucose levels were comparable.

In the insulin tolerance test, DKO mice displayed severe sensitivity to insulin, with glucose levels dropping rapidly after intraperitoneal injection of insulin (Fig. 4E). The inability of these mice to restore glucose levels is so pronounced that all the DKO mice required rescue from hypoglycemic shock and near death by injection with glucose within 1 h.

DKO mice are hyperphagic and have higher rate of whole body metabolism

Using Oxymax comprehensive animal monitoring system (CLAMS), food intake of the mice was measured. In light:dark conditions where food is available *ad libitum*, DKO mice had a higher daily food intake compared with WT (Fig. 5A). As expected, the daily food intake is lower during restricted feeding compared with feeding in both LD and DD, when the mice had access to food all the time. An exception to this is the KOH mice, which had similar food intake regardless of light and

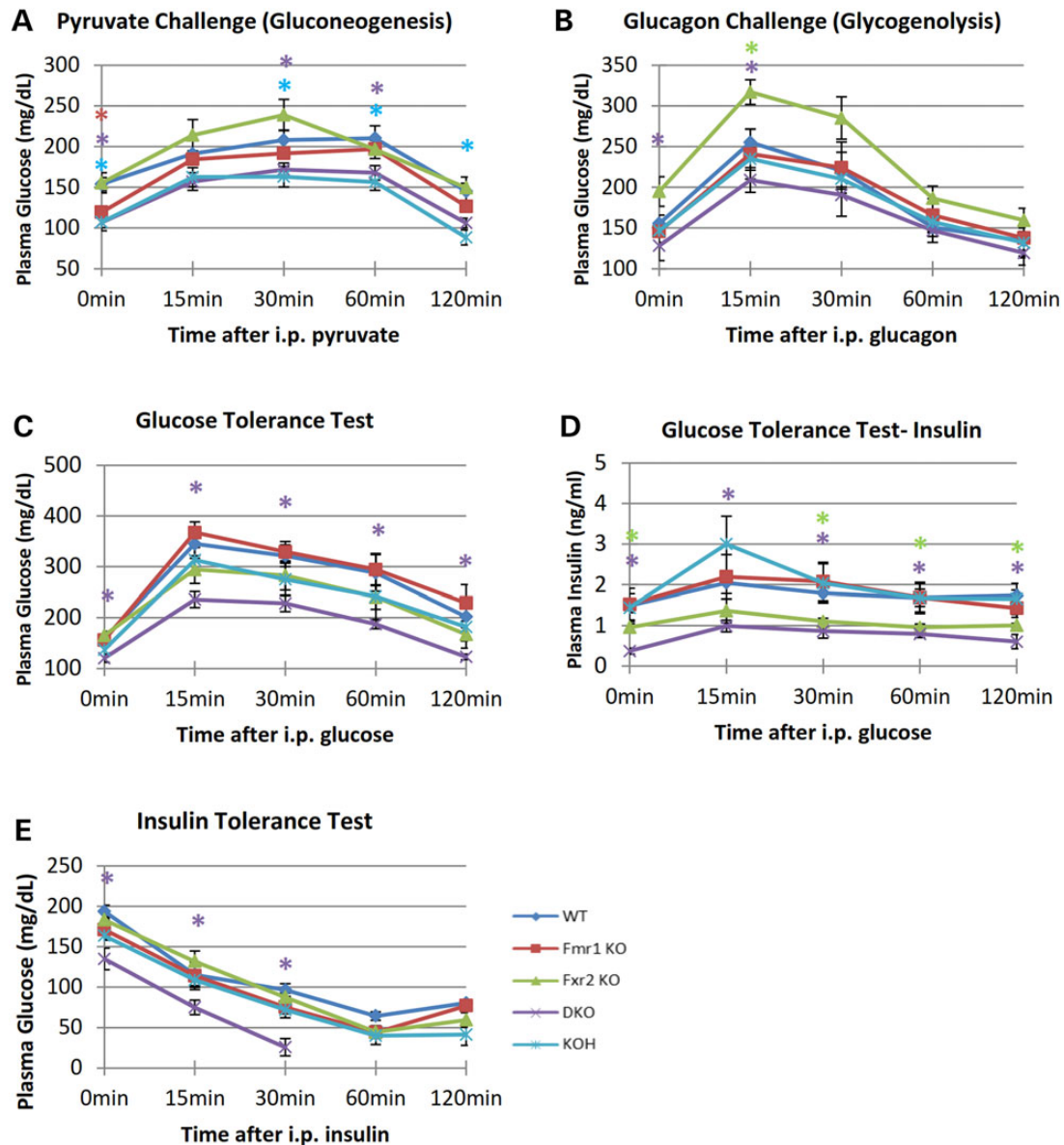


Figure 4. Impaired glucose production and responses to glucose and insulin in the DKO mice. (A) IP injection of pyruvate after overnight fasting for ~16 h. DKO and KOH mice exhibit reduced gluconeogenesis. (B) IP injection of glucagon after 6 h fasting. Glycogenolysis is diminished in DKO mice and enhanced in Fxr2 KO. (C) Glucose tolerance test after 6 h of fasting. The DKO mice exhibited enhanced efficiency at restoring blood glucose to basal levels. (D) Insulin levels measured from glucose tolerance test. DKO and Fxr2 KO mice do not show a similar response to the bolus of glucose. (E) In the insulin tolerance test, DKO mice displayed sensitivity to insulin, with pronounced inability to restore glucose levels to the point of needing to be injected with glucose by 60 min post-insulin. For A–E, age- and weight-matched mice maintained in 12:12 LD, food available *ad libitum*, all tests performed at about ZT7 (ZT0 = 7 AM). $N = 6–7$ per genotype except for C, with $N = 11–14$ per genotype. Values are presented as mean \pm SEM, differences were considered significant (*) when $P < 0.05$. Changes between time points and genotypes determined by ANOVA; pairwise comparisons of each genotype to WT by t-test.

food conditions. As with LD, the DKO mice (as well as Fxr2 KO mice) had significantly higher food intake compared with WT in DD with restricted feeding (DD-RF). Interestingly, across genotypes, daily food intake is comparable between LD and DD, suggesting that the food restriction is a more significant factor to feeding rate than light conditions.

Respiratory exchange ratio ($RER = VO_2/VCO_2$) was also measured using CLAMS. Measurements were comparable between genotypes in each of the light/feeding conditions (LD, DD and DD-RF); however, there is significant difference when RER values in DD-RF were compared with either LD or DD (Fig. 5B). Both LD and DD values are significantly higher than the values for DD-RF,

but they are themselves comparable to one another. Again, here we can deduce that restriction of food availability is a stronger factor towards metabolic imbalance than light conditions. These observations are consistent when the measurements are displayed hourly through a 24-h period (data not shown). However, while the DKO mice had RER levels comparable to that of WT mice, both the VCO_2 (carbon dioxide production) and VO_2 (oxygen consumption) levels measured for these mice are significantly higher compared with WT, in all the light/food conditions (Fig. 5C and D). These data indicate that the mutations in both Fmr1 and Fxr2 cause an increase in whole body metabolism and may help explain why these mutant mice have low fat stores even as they

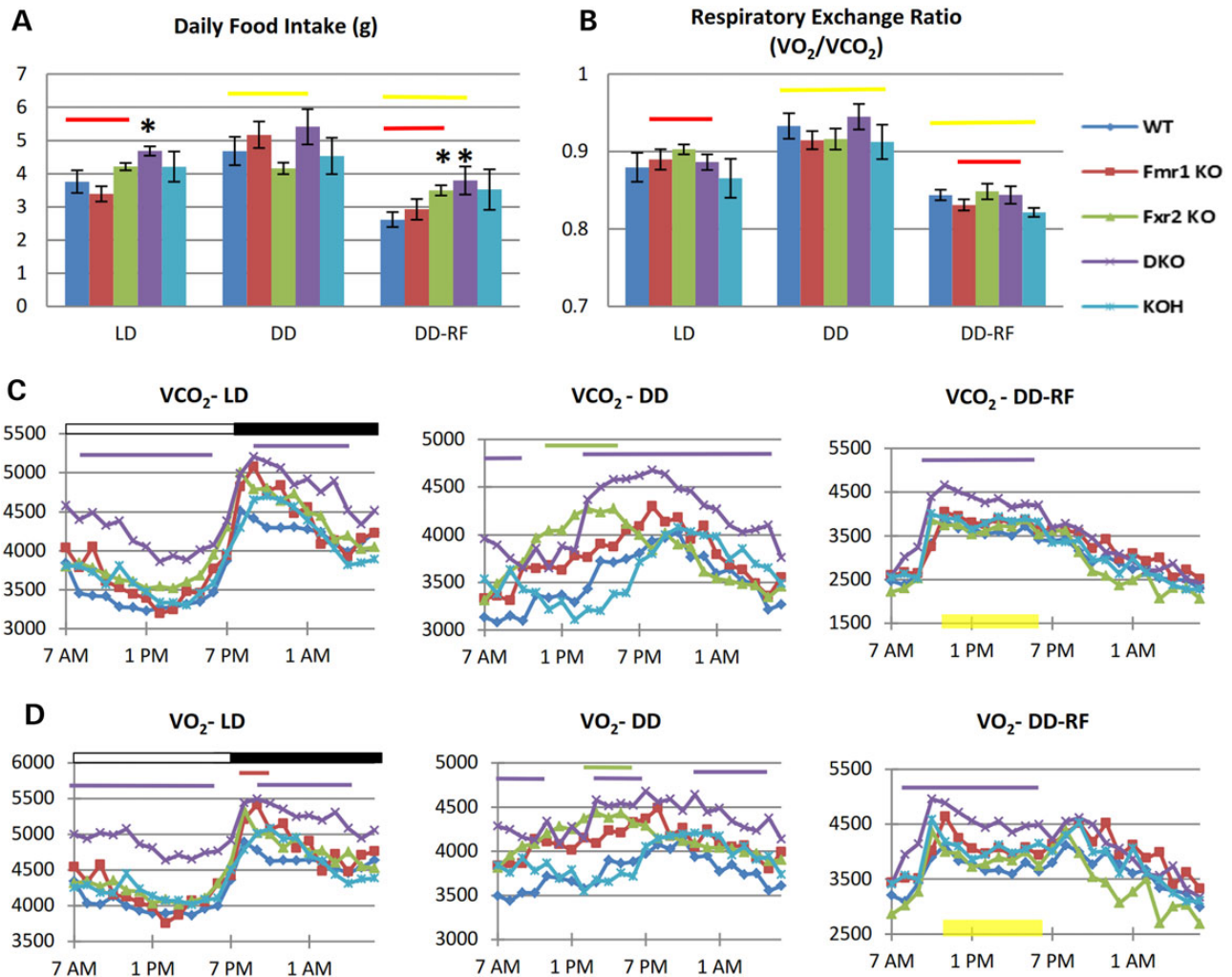


Figure 5. DKO mice have higher food intake, VCO₂ and VO₂ in LD, DD and DD-RF. CLAMS measurement, 5 days in 12:12 LD, 5 days in DD and 5 days in DD with restricted feeding. (A) Average daily food intake is increased in DKO mice in both LD and DD-RF. (B) Average daily respiratory exchange ratio (VO₂/VCO₂) is comparable between genotypes. VCO₂ (C) and VO₂ (D) levels in LD, DD and DD-RF. Genotype differences with WT are denoted by asterisks; differences between light/feeding conditions within each genotype are marked by paired orange (between LD and DD), red (between LD and DD-RF) and yellow lines (between DD and DD-RF). N = 6–9 per genotype, values are presented as mean ± SEM, differences were considered significant (*) when P < 0.05. Changes between time points and genotypes determined by ANOVA; pairwise comparisons of each genotype to the WT by t-test.

feed more. The increase in both oxygen consumption and carbon dioxide production is consistent with increased locomotor activity observed in the DKO mice (data not shown).

Levels of metabolic gene mRNAs in the liver are altered in the DKO mice

While the importance of fragile X-related proteins in mammalian circadian behaviors has been reported, and the relationship between the peripheral liver clock and metabolism has been established, there has been no evidence until now that FXRs play a role in metabolic homeostasis. We used a PCR array approach to screen genes involved in glucose homeostasis for alterations in mRNA abundance in the DKO mice. Mice were first entrained to 12:12 LD cycle, then transferred to total darkness and subjected to 2 days of restricted feeding before their livers were harvested for RNA extraction.

Out of 84 genes tested, three showed significant change in expression in livers collected at 7 AM, when mice had been fasted for

12 h. One mRNA showed up-regulation in the DKO compared with WT (*Slc2a1*, a glucose transporter), while the other two (*Pklr*, liver pyruvate kinase and the nuclear receptor *Pparg*) were down-regulated relative to WT livers (Table 1). We also looked at the expression of the same 84 genes in livers collected at 1 PM, when previously fasted mice had had access to food for 2 h. Nine additional genes showed significant differences in expression between the WT and DKO, of which four are up-regulated in the DKO and five are down-regulated (Table 1). It is worth noting that none of these genes overlap; there are completely different sets of genes that are differentially expressed at the 7 AM and 1 PM time points.

Several genes showed drastically different directions of fold change in the DKO between 7 AM and 1 PM. For example, *Fos* is up-regulated in the DKO compared with WT at 7 AM, but are then down-regulated at 1 PM when normalized to WT, while genes like *Adra1d* and *Ins1* have the opposite pattern. This demonstrates that not only is there a difference in the expression of certain metabolic genes between WT and *Fmr1/Fxr2* DKO

Table 1. Differential expression of insulin signaling genes between WT and DKO liver

Insulin signaling gene	Fold change	T-test	Fold up- or down-regulation
	DKO/WT	P-value	DKO/WT
7 AM			
<i>Pklr</i>	0.51	0.04	-1.98
<i>Pparg</i>	0.29	0.01	-3.49
<i>Slc2a1</i>	2.13	0.01	2.13
1 PM			
<i>Adra1d</i>	2.66	0.01	2.66
<i>Aebp1</i>	3.08	0.02	3.08
<i>Dok2</i>	0.52	0.05	-1.93
<i>Fbp1</i>	0.51	0.05	-1.96
<i>Fos</i>	0.50	0.05	-2.01
<i>Insl3</i>	1.74	0.03	1.74
<i>Prkcz</i>	0.74	0.02	-1.36
<i>Rps6ka1</i>	0.53	0.04	-1.88

From PCR array, expression of 84 genes was measured in the WT and DKO mice, at 7 AM and 1 PM, with the mice under total darkness and food available 11 AM–3 PM. Gene expression in DKO was normalized to WT and fold change calculated at both 7 AM and 1 PM. Genes presented are the ones where $P < 0.05$ from t-test; in each time point, 3–4 male mice 7–8 months old were used to collect liver tissue from either WT or DKO mice.

Table 2. Differential expression of insulin signaling genes between time points in the WT and DKO liver

Insulin signaling gene	Fold change	T-test	Fold up- or down-regulation
	1 PM/7 AM	P-value	1 PM/7 AM
DKO			
<i>Akt1</i>	1.56	0.05	1.56
<i>Dok1</i>	1.68	0.02	1.68
<i>Frs2</i>	1.31	0.02	1.31
<i>Gck</i>	6.88	0.0001	6.88
<i>Igfbp1</i>	0.03	0.03	-38.50
<i>Irs2</i>	0.28	0.05	-3.55
<i>Jun</i>	3.25	0.01	3.25
<i>Pik3r1</i>	2.14	0.02	2.14
WT			
<i>Akt1</i>	1.58	0.03	1.58
<i>Eif2b1</i>	1.16	0.04	1.16
<i>Fos</i>	4.31	0.03	4.31
<i>Gck</i>	6.02	0.0002	6.02
<i>Igfbp1</i>	0.07	0.01	-13.36
<i>Irs1</i>	2.30	0.03	2.30
<i>Irs2</i>	0.24	0.03	-4.16
<i>Jun</i>	3.11	0.004	3.11
<i>Map2k1</i>	1.63	0.05	1.63
<i>Nos2</i>	3.95	0.05	3.95
<i>Pik3r1</i>	3.16	0.001	3.16
<i>Prkcc</i>	0.31	0.0007	-3.25
<i>Slc2a1</i>	2.36	0.01	2.36

From PCR array, expression of 84 genes was measured in the WT and DKO mice, at 7 AM and 1 PM, with the mice under total darkness and food available 11 AM–3 PM. Change in gene expression at 1 PM relative to expression at 7 AM was calculated for both DKO and WT mice. Genes presented are the ones where $P < 0.05$ from t-test; in each time point, 3–4 male mice 7–8 months old were used to collect liver tissue from either WT or DKO mice.

mice, but these differences shift when tested at two different feeding conditions. Moreover, in each of the two genotypes, there was a significant difference in mRNA levels between the two time points (Table 2). In the DKO mice, eight genes had such a difference, two of which had significantly lower expression levels at 1 PM compared with 7 AM. The largest difference was seen in *Igfbp1*, and this is also observed in the WT, along with 12 other genes that were differentially expressed between 1 PM and 7 AM. Six genes had significant difference in expression between time points in both the WT and the DKO mice: *Akt1*, *Gck*, *Igfbp1*, *Irs2*, *Jun* and *Pik3r1*.

Discussion

The circadian clock is essential for driving daily rhythms of physiology and behavior, most importantly in the synchronization of energy storage and utilization with changes in the external environment (34–36). Numerous studies have demonstrated the impact of circadian clock gene disruption to the metabolic states of humans and animals, including the development of comorbidities such as obesity, diabetes and atherosclerosis (21–25,37–39). Moreover, several lines of evidence indicate that circadian glucose homeostasis requires a functional liver clock (23,37,40,41). Previous studies in mouse models for fragile X syndrome demonstrated that fragile X-related proteins (FXRs) are essential for maintaining circadian rhythm, and mice that are lacking in both *Fmr1p* and *Fxr2p* have disrupted cycling of clock components in the liver (16).

Prompted by the hypothesis that FXRs are important regulators of metabolism through their roles in maintaining circadian rhythm, we sought to profile the metabolic state of mice that are lacking in one or more FXR genes. We found that the *Fmr1/Fxr2* DKO mice have an impaired metabolic state, including having significantly low amounts of fat, hypoglycemia and sensitivity to insulin. These results are contradictory to phenotypes found in mice with mutations in the *Clock* and *Bmal1* genes, which resemble the human metabolic syndrome (predisposition to obesity, hyperglycemia and hyperlipidemia) but are consistent with observations from studies where the liver clock is specifically ablated (22–24). This is expected since the DKO mutant mice have intact function in the central clock and only demonstrate impaired rhythm in the liver clock (16). It is also possible that most of the impairments in glucose homeostasis are secondary phenotypes that arise from the low amount of fat stored in the DKO mice. This certainly appears to be true for certain phenotypes such as the low levels of leptin in circulating plasma, but the DKO mice had several metabolic impairments that were not seen in the *Fxr2* KO mice, which had comparable levels of fat content. Most notable of these are the circadian cycling of glucose and insulin during restricted feeding and the response to injected insulin.

A result that is also noteworthy is that the mice lacking only *Fmr1* had phenotypes comparable to WT except for lower levels of plasma insulin when subjected to total darkness. This was also true for *Fmr1* KO; *Fxr2* het mice (KOH), but these mice showed an additional deficiency in gluconeogenesis. Taken together, the differences in the metabolic phenotypes among the different FXR mutants demonstrate that the more severe metabolic defects only manifest when there is a mutation in both *Fmr1* and *Fxr2*, even as a mutation in either gene produces some form of metabolic impairment. Given the structural similarities and overlaps in localization and functions of the FXRs, it has been postulated that *Fxr2p* can, at least partially, compensate for the loss of *Fmrp* (19,42), and our prior data comparing DKO

mice in circadian behavior and hippocampal electrophysiology support this notion (16,20). The data in this study strongly suggest a cooperative effect of *Fmr1* and *Fxr2* on gene expression in the liver, where loss of both together results in a much more pronounced phenotype.

Metabolic anomalies including increased glucose uptake and excess protein synthesis in brain have been reported in *Fmr1* KO mice, while in the fly it has been shown that FMRP is required during brain development and may function in neuroblast reactivation by regulating an output of the insulin signaling pathway (43–47). Interestingly, El Idrissi *et al.* noted a significant decrease in the number of islets of Langerhans in the pancreas of *Fmr1* KO mice, along with reductions in somatostatin and glucagon immunoreactivity per islet (46). Future studies of pancreas structure and function in the mice analyzed here are warranted. Males with fragile X syndrome also show cerebral glucose metabolic changes and a fraction develops hyperphagia and obesity ('Prader-Willi like') but are rarely found to progress to diabetes (17,18,44,48). Metabolic profiling in mice revealed profound consequences of *Fmr1* deficiency in brain metabolism, which in turn lead to alterations in the metabolic response in fragile X, along with anomalies in other physiological processes (49). These data suggest that metabolic issues may extend to other tissue types, including the brain, and may contribute to some of the behavioral and cognitive features of the disorder.

In a screen comparing liver mRNA from WT and DKO mice, we found differential expression of several genes involved in glucose homeostasis. Of these 12 genes, only *Fos* has been previously linked to Fragile X Syndrome, through its role in stress response in the brain (50). Also of particular note is *Pparg*, which is already known to link circadian rhythm and metabolism and is a key regulator of adipocyte differentiation (51, 52). While PPAR γ has not yet been shown to interact with or be regulated by either *Fmrp* or *Fxr2p*, it regulates *Bmal1*, either through direct coupling or via its negative regulator *Rev-erb α* , or both, and is directly regulated by another clock gene, *Per2* (53, 54). Apart from the differential expression between DKO and WT, 16 of the 84 glucose homeostasis genes tested were also differentially expressed between time points, wherein the mice have been fasted in one time point (7 AM) and re-fed at the other (1 PM). These include six genes that had the same feeding-induced differences in expression in both the WT and DKO mice, most of which are involved in insulin signaling (*Akt*, *Pik3r1*, *Igf1bp1*, *Irs2*).

Our findings demonstrate an additional function for fragile X-related genes. This important role in metabolism underscores not just the close integration of circadian and metabolic systems, but is one that is possibly linked to learning and memory. Further investigation of the mechanism(s) by which FXRs participate in regulating glucose homeostasis may lead to improved understanding of the relationships between cognition, food and circadian rhythm.

Materials and Methods

Mice and housing conditions

All experiments were performed with male C57BL/6J mice of the following genotypes: *Fmr1* KO, *Fxr2* KO, *Fmr1/Fxr2* double KO (DKO) and *Fmr1* KO/*Fxr2* heterozygous (KOH), along with their wild-type littermates as controls. The mice were 5–6 months old at the start of the experiments. Unless otherwise indicated, mice were individually housed for the duration of the experiments, under 12 h light:12 h dark conditions (12:12 LD) with the lights on from 7 AM to 7 PM and with food (standard laboratory chow,

Harlan Teklad, Wisconsin) and water available *ad libitum*. Where restricted feeding is performed, food availability is restricted to 8 h on the first day of experiment (11 AM–7 PM) and is reduced by an hour each day until food availability is down to 4 h (11 AM–3 PM). All experiments were conducted in accordance with the NIH *Guide for the Use and Care of Laboratory Animals* and approved by the Institutional Animal Care and Use Committee of Baylor College of Medicine.

EchoMRI and assay methods

Magnetic resonance imaging (MRI) was performed on conscious, live mice 5–6 months old using an EchoMRI™ whole body composition analyzer (Echo Medical Systems). For analysis of metabolic markers, tail blood was collected over 24 h at four time points (ZT0, ZT6, ZT12 and ZT18 where ZT0 is subjective day beginning at 7 AM) using heparin-coated tubes. Plasma was obtained immediately by centrifugation and then analyzed for glucose, triglycerides and cholesterol using standard reagents from Thermo Scientific; insulin, leptin and adiponectin using ELISA kit from Millipore; free fatty acids using reagents from WACO Chemicals; and glycerol using reagents from Sigma. On collection days for DD-RF, food is available between 11 AM and 6 PM.

Intraperitoneal injection for tolerance tests

Age- and weight-matched mice were fasted and injected intraperitoneally with test substance. To test rate of gluconeogenesis, pyruvate was injected after overnight fasting for ~16 h, dosage 2 g/kg of body weight. To test glycogenolysis, glucagon was injected after mice were fasted for 6 h, dosage 10 μ g/g body weight. Glucose tolerance test was performed after 6 h of fasting at a dosage 1.5 mg/g of body weight, while insulin tolerance was tested after 4 h of fasting, using a dosage 1 mU/g of body weight. For all tests, blood samples were taken by tail venesection at 0 min (just before injection) and at 15, 30, 60 and 120 min post-injection. Injections were performed at ZT7 (ZT0 is 7 AM). Glucose and insulin were measured as described above. Mice were given only water during the tests.

Indirect calorimetry and food intake

Metabolic rate and food intake were determined by Oxymax comprehensive lab animal monitoring system (Columbus Instruments, Ohio). Following 1 week of acclimation, food intake and energy expenditure were recorded continuously for 5 days in LD followed by 5 days in DD with food *ad libitum* and then another 5 days in DD with restricted feeding.

PCR array

Male WT and DKO mice 7–8 months old were transferred to total darkness, and the food availability was restricted. On Day 2 of restricted feeding (food available 11 AM–6 PM), the animals were sacrificed via cervical dislocation, one group sacrificed at 7 AM and another at 1 PM. Tissues were removed immediately and flash frozen in liquid nitrogen. Briefly, ~30 mg liver tissue was homogenized in 2 ml TRIzol using Polytron homogenizer, and total RNA was extracted using Qiagen RNeasy Mini Kit and DNase Clean-up according to manufacturer's instructions. The concentration and purity of RNA were determined by absorbance at 260/280 nm, and 0.5 μ g of RNA was used to generate cDNA using Qiagen RT² First Strand Kit. A PCR screening array for 84 genes in the mouse insulin signaling was conducted (RT² Profiler PCR Array; Qiagen

Catalog no. PAMM-030ZC), running the reactions on an ABI 7900HT Fast System SDS (Applied Biosystems) machine using SYBR Green ROX qPCR Mastermix (Qiagen). PCR array data were calculated by the comparative cycle threshold method, normalized against multiple housekeeping genes, and expressed as mean fold change in DKO samples relative to WT control samples. In each time point, 3–4 animals per genotype were used as biological replicates.

Statistical analyses

Unless stated otherwise, data are presented as means with standard error of means. Analyses for the significance of differences were performed using analysis of variance (ANOVA). Pairwise comparisons of each genotype to the WT were made using two-tailed Student's *t*-test assuming unequal variances ($P < 0.05$).

Acknowledgements

We thank Drs Rodney Samaco and Yanghong Gu for technical advice and Michael Gayton for assistance with statistical analyses. We thank the Mouse Metabolism Core at Baylor College of Medicine.

Conflict of Interest statement. None declared.

Funding

This work was supported in part by the FRAXA Research Foundation and National Institutes of Health (NIH) grants (NS051630, HD24064, NS67461).

References

1. Peprah, E. (2012) Fragile X syndrome: the FMR1 CGG repeat distribution among world populations. *Ann. Hum. Genet.*, **76**, 178–191.
2. Hantash, F.M., Goos, D.M., Crossley, B., Anderson, B., Zhang, K., Sun, W. and Strom, C.M. (2011) FMR1 premutation carrier frequency in patients undergoing routine population-based carrier screening: insights into the prevalence of fragile X syndrome, fragile X-associated tremor/ataxia syndrome, and fragile X-associated primary ovarian insufficiency in the United States. *Genet. Med.*, **13**, 39–45.
3. Verkerk, A.J., Pieretti, M., Sutcliffe, J.S., Fu, Y.H., Kuhl, D.P., Pizutti, A., Reiner, O., Richards, S., Victoria, M.F., Zhang, F.P. et al. (1991) Identification of a gene (FMR-1) containing a CGG repeat coincident with a breakpoint cluster region exhibiting length variation in fragile X syndrome. *Cell*, **65**, 905–914.
4. Zhang, Y., O'Connor, J.P., Siomi, M.C., Srinivasan, S., Dutra, A., Nussbaum, R.L. and Dreyfuss, G. (1995) The fragile X mental retardation syndrome protein interacts with novel homologs FXR1 and FXR2. *EMBO J.*, **14**, 5358–5366.
5. Darnell, J.C., Fraser, C.E., Mostovetsky, O. and Darnell, R.B. (2009) Discrimination of common and unique RNA-binding activities among Fragile X mental retardation protein paralogs. *Hum. Mol. Genet.*, **18**, 3164–3177.
6. Ascano, M. Jr, Mukherjee, N., Bandaru, P., Miller, J.B., Nussbaum, J.D., Corcoran, D.L., Langlois, C., Munschauer, M., DeWelle, S., Hafner, M. et al. (2012) FMRP targets distinct mRNA sequence elements to regulate protein expression. *Nature*, **492**, 382–386.
7. Kirkpatrick, L.L., McIlwain, K.A. and Nelson, D.L. (2001) Comparative genomic sequence analysis of the FXR gene family: FMR1, FXR1, and FXR2. *Genomics*, **78**, 169–177.
8. Davidovic, L., Durand, N., Khalfallah, O., Tabet, R., Barbry, P., Mari, B., Sacconi, S., Moine, H. and Bardoni, B. (2013) A novel role for the RNA-binding protein FXR1P in myoblasts cell-cycle progression by modulating p21/Cdkn1a/Cip1/Waf1 mRNA stability. *PLoS Genet.*, **9**, e1003367.
9. Whitman, S.A., Cover, C., Yu, L., Nelson, D.L., Zarnescu, D.C. and Gregorio, C.C. (2011) Desmoplakin and talin2 are novel mRNA targets of fragile X-related protein-1 in cardiac muscle. *Circ. Res.*, **109**, 262–271.
10. Gould, E.L., Loesch, D.Z., Martin, M.J., Hagerman, R.J., Armstrong, S.M. and Huggins, R.M. (2000) Melatonin profiles and sleep characteristics in boys with fragile X syndrome: a preliminary study. *Am. J. Med. Genet.*, **95**, 307–315.
11. Kronk, R., Bishop, E.E., Raspa, M., Bickel, J.O., Mandel, D.A. and Bailey, D.B., Jr. (2010) Prevalence, nature, and correlates of sleep problems among children with fragile X syndrome based on a large scale parent survey. *Sleep*, **33**, 679–687.
12. Kronk, R., Dahl, R. and Noll, R. (2009) Caregiver reports of sleep problems on a convenience sample of children with fragile X syndrome. *Am. J. Intellect. Dev. Disabil.*, **114**, 383–392.
13. Miano, S., Bruni, O., Elia, M., Scifo, L., Smerieri, A., Trovato, A., Verrillo, E., Terzano, M.G. and Ferri, R. (2008) Sleep phenotypes of intellectual disability: a polysomnographic evaluation in subjects with Down syndrome and Fragile-X syndrome. *Clin. Neurophysiol.*, **119**, 1242–1247.
14. Bushey, D., Tononi, G. and Cirelli, C. (2009) The Drosophila fragile X mental retardation gene regulates sleep need. *J. Neurosci.*, **29**, 1948–1961.
15. Inoue, S., Shimoda, M., Nishinokubi, I., Siomi, M.C., Okamura, M., Nakamura, A., Kobayashi, S., Ishida, N. and Siomi, H. (2002) A role for the Drosophila fragile X-related gene in circadian output. *Curr. Biol.*, **12**, 1331–1335.
16. Zhang, J., Fang, Z., Jud, C., Vansteensel, M.J., Kaasik, K., Lee, C.C., Albrecht, U., Tamanini, F., Meijer, J.H., Oostra, B.A. et al. (2008) Fragile X-related proteins regulate mammalian circadian behavioral rhythms. *Am. J. Hum. Genet.*, **83**, 43–52.
17. de Vries, B.B., Fryns, J.P., Butler, M.G., Canziani, F., Wesby-van Swaay, E., van Hemel, J.O., Oostra, B.A., Halley, D.J. and Niermeijer, M.F. (1993) Clinical and molecular studies in fragile X patients with a Prader-Willi-like phenotype. *J. Med. Genet.*, **30**, 761–766.
18. Nowicki, S.T., Tassone, F., Ono, M.Y., Ferranti, J., Croquette, M.F., Goodlin-Jones, B. and Hagerman, R.J. (2007) The Prader-Willi phenotype of fragile X syndrome. *J. Dev. Behav. Pediatr.*, **28**, 133–138.
19. Spencer, C.M., Serysheva, E., Yuva-Paylor, L.A., Oostra, B.A., Nelson, D.L. and Paylor, R. (2006) Exaggerated behavioral phenotypes in Fmr1/Fxr2 double knockout mice reveal a functional genetic interaction between Fragile X-related proteins. *Hum. Mol. Genet.*, **15**, 1984–1994.
20. Zhang, J., Hou, L., Klann, E. and Nelson, D.L. (2009) Altered hippocampal synaptic plasticity in the FMR1 gene family knockout mouse models. *J. Neurophysiol.*, **101**, 2572–2580.
21. Rudic, R.D., McNamara, P., Curtis, A.M., Boston, R.C., Panda, S., Hogenesch, J.B. and Fitzgerald, G.A. (2004) BMAL1 and CLOCK, two essential components of the circadian clock, are involved in glucose homeostasis. *PLoS Biol.*, **2**, e377.
22. Marcheiva, B., Ramsey, K.M., Buhr, E.D., Kobayashi, Y., Su, H., Ko, C.H., Ivanova, G., Omura, C., Mo, S., Vitaterna, M.H. et al. (2010) Disruption of the clock components CLOCK and BMAL1 leads to hypoinsulinaemia and diabetes. *Nature*, **466**, 627–631.
23. Lamia, K.A., Storch, K.F. and Weitz, C.J. (2008) Physiological significance of a peripheral tissue circadian clock. *Proc. Natl Acad. Sci. USA*, **105**, 15172–15177.

24. Kennaway, D.J., Varcoe, T.J., Voultzios, A. and Boden, M.J. (2013) Global loss of *bmal1* expression alters adipose tissue hormones, gene expression and glucose metabolism. *PLoS ONE*, **8**, e65255.
25. Milagro, F.I., Gomez-Abellan, P., Campion, J., Martinez, J.A., Ordovas, J.M. and Garaulet, M. (2012) CLOCK, PER2 and BMAL1 DNA methylation: association with obesity and metabolic syndrome characteristics and monounsaturated fat intake. *Chronobiol. Int.*, **29**, 1180–1194.
26. Paik, K.H., Jin, D.K., Song, S.Y., Lee, J.E., Ko, S.H., Song, S.M., Kim, J.S., Oh, Y.J., Kim, S.W., Lee, S.H. et al. (2004) Correlation between fasting plasma ghrelin levels and age, body mass index (BMI), BMI percentiles, and 24-hour plasma ghrelin profiles in Prader-Willi syndrome. *J. Clin. Endocrinol. Metab.*, **89**, 3885–3889.
27. Powell, W.T., Coulson, R.L., Crary, F.K., Wong, S.S., Ach, R.A., Tsang, P., Alice Yamada, N., Yasui, D.H. and Lasalle, J.M. (2013) A Prader-Willi locus lncRNA cloud modulates diurnal genes and energy expenditure. *Hum. Mol. Genet.*, **22**, 4318–4328.
28. Smith, A.C., Gropman, A.L., Bailey-Wilson, J.E., Goker-Alpan, O., Elsea, S.H., Blancato, J., Lupski, J.R. and Potocki, L. (2002) Hypercholesterolemia in children with Smith-Magenis syndrome: del (17) (p11.2p11.2). *Genet. Med.*, **4**, 118–125.
29. Lalaria, M., Saha, P., Potocki, L., Bi, W., Yan, J., Girirajan, S., Burns, B., Elsea, S., Walz, K., Chan, L. et al. (2012) A duplication CNV that conveys traits reciprocal to metabolic syndrome and protects against diet-induced obesity in mice and men. *PLoS Genet.*, **8**, e1002713.
30. Burns, B., Schmidt, K., Williams, S.R., Kim, S., Girirajan, S. and Elsea, S.H. (2010) *Rai1* haploinsufficiency causes reduced *Bdnf* expression resulting in hyperphagia, obesity and altered fat distribution in mice and humans with no evidence of metabolic syndrome. *Hum. Mol. Genet.*, **19**, 4026–4042.
31. Flore, P., Bricout, V.A., van Biesen, D., Guinot, M., Laporte, F., Pepin, J.L., Eberhard, Y., Favre-Juvin, A., Wuyam, B., van de Vliet, P. et al. (2008) Oxidative stress and metabolism at rest and during exercise in persons with Down syndrome. *Eur. J. Cardiovasc. Prev. Rehabil.*, **15**, 35–42.
32. Lott, I.T. (2012) Neurological phenotypes for Down syndrome across the life span. *Prog. Brain Res.*, **197**, 101–121.
33. Rohrer, T.R., Hennes, P., Thon, A., Dost, A., Grabert, M., Rami, B., Wiegand, S. and Holl, R.W. (2010) Down's syndrome in diabetic patients aged <20 years: an analysis of metabolic status, glycaemic control and autoimmunity in comparison with type 1 diabetes. *Diabetologia*, **53**, 1070–1075.
34. Li, J.D., Hu, W.P. and Zhou, Q.Y. (2012) The circadian output signals from the suprachiasmatic nuclei. *Prog. Brain Res.*, **199**, 119–127.
35. Sahar, S. and Sassone-Corsi, P. (2012) Regulation of metabolism: the circadian clock dictates the time. *Trends Endocrinol. Metab.*, **23**, 1–8.
36. Eckel-Mahan, K. and Sassone-Corsi, P. (2013) Metabolism and the circadian clock converge. *Physiol. Rev.*, **93**, 107–135.
37. Lee, J., Kim, M.S., Li, R., Liu, V.Y., Fu, L., Moore, D.D., Ma, K. and Yeheer, V.K. (2011) Loss of *Bmal1* leads to uncoupling and impaired glucose-stimulated insulin secretion in beta-cells. *Islets*, **3**, 381–388.
38. Sadacca, L.A., Lamia, K.A., deLemos, A.S., Blum, B. and Weitz, C.J. (2011) An intrinsic circadian clock of the pancreas is required for normal insulin release and glucose homeostasis in mice. *Diabetologia*, **54**, 120–124.
39. Paschos, G.K., Ibrahim, S., Song, W.L., Kunieda, T., Grant, G., Reyes, T.M., Bradfield, C.A., Vaughan, C.H., Eiden, M., Masoodi, M. et al. (2012) Obesity in mice with adipocyte-specific deletion of clock component *Arntl*. *Nat. Med.*, **18**, 1768–1777.
40. Kornmann, B., Schaad, O., Bujard, H., Takahashi, J.S. and Schibler, U. (2007) System-driven and oscillator-dependent circadian transcription in mice with a conditionally active liver clock. *PLoS Biol.*, **5**, e34.
41. Lee, J., Moulik, M., Fang, Z., Saha, P., Zou, F., Xu, Y., Nelson, D.L., Ma, K., Moore, D.D. and Yeheer, V.K. (2013) *Bmal1* and beta-cell clock are required for adaptation to circadian disruption, and their loss of function leads to oxidative stress-induced beta-cell failure in mice. *Mol. Cell. Biol.*, **33**, 2327–2338.
42. Agulhon, C., Blanchet, P., Kobetz, A., Marchant, D., Faucon, N., Sarda, P., Moraine, C., Sittler, A., Biancalana, V., Malafosse, A. et al. (1999) Expression of *FMR1*, *FXR1*, and *FXR2* genes in human prenatal tissues. *J. Neuropathol. Exp. Neurol.*, **58**, 867–880.
43. Qin, M., Kang, J. and Smith, C.B. (2005) A null mutation for *Fmr1* in female mice: effects on regional cerebral metabolic rate for glucose and relationship to behavior. *Neuroscience*, **135**, 999–1009.
44. Qin, M., Kang, J. and Smith, C.B. (2002) Increased rates of cerebral glucose metabolism in a mouse model of fragile X mental retardation. *Proc. Natl Acad. Sci. USA*, **99**, 15758–15763.
45. Callan, M.A., Clements, N., Ahrendt, N. and Zarnescu, D.C. (2012) Fragile X Protein is required for inhibition of insulin signaling and regulates glial-dependent neuroblast reactivation in the developing brain. *Brain Res.*, **1462**, 151–161.
46. El Idrissi, A., Yan, X., Sidime, F. and L'Amoreaux, W. (2010) Neuro-endocrine basis for altered plasma glucose homeostasis in the Fragile X mouse. *J. Biomed. Sci.*, **17** (Suppl. 1), S8.
47. Qin, M., Schmidt, K.C., Zametkin, A.J., Bishu, S., Horowitz, L.M., Burlin, T.V., Xia, Z., Huang, T., Quezado, Z.M. and Smith, C.B. (2013) Altered cerebral protein synthesis in fragile X syndrome: studies in human subjects and knockout mice. *J. Cereb. Blood Flow Metab.*, **33**, 499–507.
48. De Vries, B.B. and Niermeijer, M.F. (1994) The Prader-Willi-like phenotype in fragile X patients: a designation facilitating clinical (and molecular) differential diagnosis. *J. Med. Genet.*, **31**, 820.
49. Davidovic, L., Navratil, V., Bonaccorso, C.M., Catania, M.V., Bardoni, B. and Dumas, M.E. (2011) A metabolomic and systems biology perspective on the brain of the fragile X syndrome mouse model. *Genome Res.*, **21**, 2190–2202.
50. Lauterborn, J.C. (2004) Stress induced changes in cortical and hypothalamic *c-fos* expression are altered in fragile X mutant mice. *Brain Res. Mol. Brain Res.*, **131**, 101–109.
51. Yang, G., Jia, Z., Aoyagi, T., McClain, D., Mortensen, R.M. and Yang, T. (2012) Systemic PPARgamma deletion impairs circadian rhythms of behavior and metabolism. *PLoS ONE*, **7**, e38117.
52. Kawai, M. and Rosen, C.J. (2010) PPARgamma: a circadian transcription factor in adipogenesis and osteogenesis. *Nat. Rev. Endocrinol.*, **6**, 629–636.
53. Wang, N., Yang, G., Jia, Z., Zhang, H., Aoyagi, T., Soodvilai, S., Symons, J.D., Schnermann, J.B., Gonzalez, F.J., Litwin, S.E. et al. (2008) Vascular PPARgamma controls circadian variation in blood pressure and heart rate through *Bmal1*. *Cell Metab.*, **8**, 482–491.
54. Grimaldi, B., Bellet, M.M., Katada, S., Astarita, G., Hirayama, J., Amin, R.H., Granneman, J.G., Piomelli, D., Leff, T. and Sassone-Corsi, P. (2010) PER2 controls lipid metabolism by direct regulation of PPARgamma. *Cell Metab.*, **12**, 509–520.